

# High Capacity Functionalized Protein Superabsorbents from an Agricultural Co-Product: A Cradle-to-Cradle Approach

Antonio Jose Capezza,\* Yuxiao Cui, Keiji Numata, Malin Lundman, William Roy Newson, Richard Tobias Olsson, Eva Johansson, and Mikael Stefan Hedenqvist\*

Synthesis of superabsorbent particles from nontoxic wheat gluten (WG) protein, as an industrial co-product, is presented. A natural molecular cross-linker named genipin (a hydrogenated glycoside) is used together with a dianhydride (ethylenediaminetetraacetic EDTAD), to enable the preparation of a material with a network structure capable of swelling up to  $\approx 4000\%$  in water and  $\approx 600\%$  in saline solution. This represents an increase in swelling by over 10 times compared to the already highly absorbing gluten reference material. The carboxylation (using EDTAD) and the cross-linking of the protein result in a hydrogel with liquid retention capacity as high as 80% of the absorbed water remaining in the WG network on extensive centrifugation, which is higher than that of commercial fossil-based superabsorbents. The results also show that more polar forms of the reacted genipin are more effectively grafted onto the protein, contributing to the swelling and liquid retention. Microscopy of the materials reveals extensive nanoporosity (300 nm), contributing to rapid capillarity-driven absorption. The use of proteins from agricultural industries for the fabrication of sustainable protein superabsorbents is herein described as an emerging avenue for the development of the next generation daily-care products with a minimal environmental impact.

chains and the fact that the proteins are available as co-products from the agricultural industry make them attractive in SAP applications for replacing their petroleum-based counterparts. The diversity of the protein constituents also makes them interesting as compared to other natural polymers such as polysaccharides.<sup>[3–10]</sup> The chemical modification of proteins via acylation has here been acknowledged as one of the more promising techniques for the functionalization of proteins toward superabsorbency.<sup>[1,3,5,11–15]</sup> The derived charged carboxylic acid groups in the polypeptide chains, from the use of ethylenediaminetetraacetic dianhydride (EDTAD), has resulted in dried protein materials with a swelling capacity sufficient to replace petroleum-based SAP.<sup>[3]</sup> EDTAD is used as an acylation agent due to its high reactivity from dilute aqueous solutions, in addition to its nontoxic nature.<sup>[3,7]</sup> The acylation from dilute aqueous solutions is a key to carry out protein modifications

without inducing extensive cross-linking, thus avoiding a limited swelling capacity of the treated proteins.<sup>[3,7,15–18]</sup>

Wheat gluten (WG) is particularly interesting as a protein material since it is a co-product from the starch industry, with the ability to perform as an absorbent material.<sup>[19–25]</sup> The

## 1. Introduction

Proteins have been demonstrated as a natural raw material for the production of superabsorbent polymers (SAP).<sup>[1,2]</sup> The richness of different functional groups along the protein molecular

A. J. Capezza, Dr. Y. Cui, Prof. R. T. Olsson, Prof. M. S. Hedenqvist  
Department of Fibre and Polymer Technology  
Polymeric Materials Division  
KTH Royal Institute of Technology  
School of Engineering Sciences in Chemistry  
Biotechnology and Health  
Stockholm 10044, Sweden  
E-mail: ajcv@kth.se; mikaelhe@kth.se

 The ORCID identification number(s) for the author(s) of this article can be found under <https://doi.org/10.1002/adsu.202000110>.

© 2020 The Authors. Published by WILEY-VCH Verlag GmbH & Co. KGaA, Weinheim. This is an open access article under the terms of the Creative Commons Attribution-NonCommercial License, which permits use, distribution and reproduction in any medium, provided the original work is properly cited and is not used for commercial purposes.

DOI: 10.1002/adsu.202000110

A. J. Capezza, Dr. W. R. Newson, Prof. E. Johansson  
Department of Plant Breeding  
Faculty of Landscape Planning  
Horticulture and Crop Production Sciences  
SLU Swedish University of Agricultural Sciences  
Alnarp 23053, Sweden  
Prof. K. Numata  
Department of Material Chemistry  
Graduate School of Engineering  
Kyoto University  
Kyotodaigaku Katsura, Nishikyo-ku, Kyoto 615-8510, Japan  
Prof. K. Numata  
Biomacromolecules Research Team  
RIKEN Center for Sustainable Resource Science  
2-1 Hirosawa, Wako, Saitama 351-0198, Japan  
M. Lundman  
Essity Hygiene and Health AB  
Gothenburg SE-405 03, Sweden

synthesis of bio-based SAPs using EDTAD-acylation in concentrated solutions has previously been reported for WG protein co-product with limitations on the absorption/swelling capacity due to insufficient formation of a protein molecular network.<sup>[26]</sup> At the same time, it has however been demonstrated that the swelling kinetics of the WG system can be modified by the addition of protein cross-linkers.<sup>[1,2,27]</sup> Here, aldehyde cross-linking agents for proteins have been used although they are regarded as toxic, e.g. glutaraldehyde, which accordingly does not make them the preferred choice in the targeted application area for SAPs in human daily-care products.<sup>[28,29]</sup> Importantly, green alternative cross-linkers do exist and as an example, the natural nontoxic cross-linker genipin (GEN), a glycoside derivate from the fruit of the plant *Gardenia Jasminoides* Ellis,<sup>[30,31]</sup> can effectively increase the water swelling capacity of WG foams at only 1 wt% concentration.<sup>[27]</sup> Previously, GEN has been used for cross-linking polysaccharides and blends with proteins (e.g., gelatin) due to the GEN bifunctional reactive structure, nontoxicity, and water solubility.<sup>[32–34]</sup>

In this study, a combined WG EDTAD-acylation protocol based on the use of GEN in dilute aqueous solutions is presented, resulting in water swelling capacity reaching  $40 \text{ g g}^{-1}$  (4000%) in 24 h, being the highest reported for this protein SAP. The addition of 4 wt% GEN not only provided a sufficient protein cross-linking for the WG EDTAD-treated protein to form a stable network in contact with water but also increased the saline and defibrinated sheep blood absorption of 600% and 250%, respectively. The centrifugation of the EDTAD/GEN WG hydrogels revealed a liquid retention capacity of 80%, which is higher than commercial synthetic SAPs encountered in disposable daily-care products. The utilization of bio-based and/or nontoxic reagents, combined with WG as inexpensive biodegradable protein raw material contributes to the formulation of bio-based SAPs that in the future are envisioned to replace the petroleum-derived SAPs in current disposable daily-care products such as diapers.

## 2. Results and Discussion

### 2.1. Swelling Properties

The water swelling capacity of WG (pristine powder) and WG/Ref (WG with no EDTAD) were similar and low (less than  $3 \text{ g}$  of water and saline per gram of dry powder ( $\text{g g}^{-1}$ ), Figure 1). The use of EDTAD yielded a material that absorbed a maximum of  $6 \text{ g g}^{-1}$  of water (WG/25ED, Figure 1a). However, the swollen material was not stable and most of it leaked out from the teabag as shown previously in a WG-EDTAD acylated material (Figure 1c-2).<sup>[26]</sup> In contrast, the addition of 4 wt% GEN after the EDTAD acylation (WG25ED4GEN) demonstrated the ability of GEN to cross-link the acylated WG to such an extent that the protein formed a stable hydrogel even after 24 h of swelling in water (Figure 1c-3). It should be noted that lower contents of GEN tested initially (0.1 and 1 wt%) did not lead to a sufficiently stable gel (not shown). The average water uptake by the WG25ED4GEN sample was 24 and  $36 \text{ g g}^{-1}$  after 30 min and 24 h immersion, respectively (Figure 1a), representing the highest reported swelling for WG-based

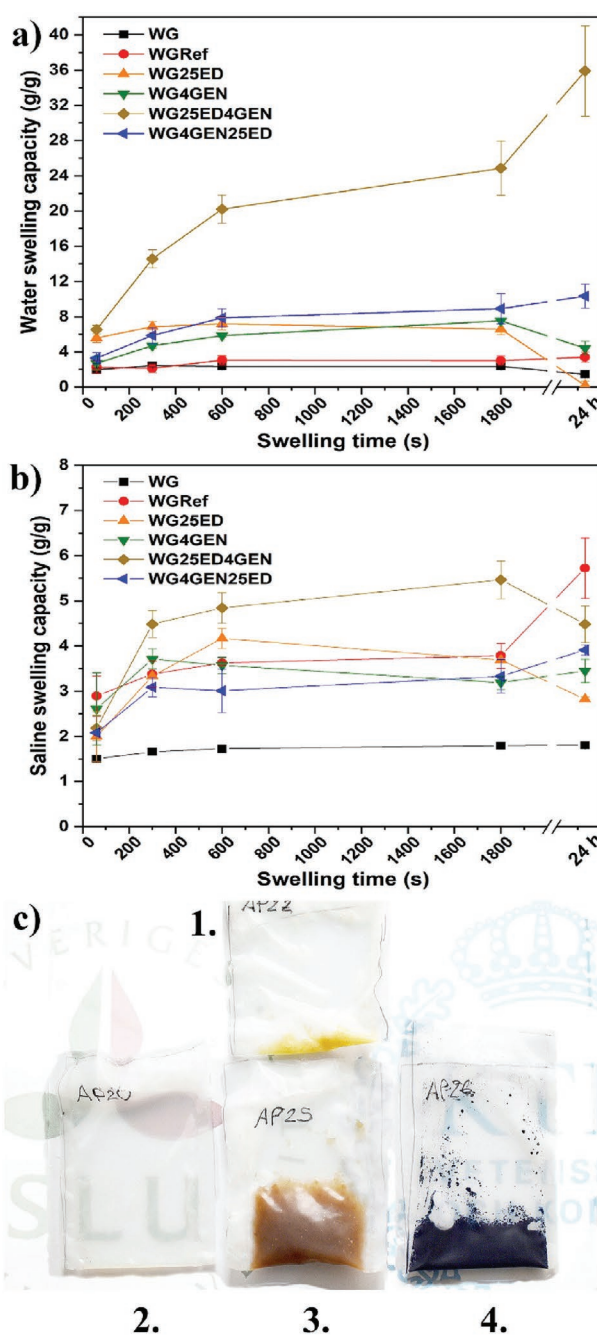


**Figure 1.** Free swelling capacity (FSC) of the different samples in water (a) and saline (b) using the tea-bag method. Representative tea bags containing WGRef, WG25ED, WG25ED4GEN, and WG4GEN25ED (1-4, respectively) after 24 h swelling in water (c).

superabsorbent materials.<sup>[1]</sup> In contrast, the addition of GEN before EDTAD (WG4GEN25ED) led to a material that reached only  $8 \text{ g g}^{-1}$  of water absorption (Figure 1a). The uptake was, however, slightly higher than that for WG4GEN (only 4 wt% GEN), which was expected as GEN will extensively cross-link the protein molecules mainly through the lysine groups.<sup>[30,35]</sup> The slight increase in the swelling of the WG4GEN25ED sample, compared to WG4GEN (without a following acylation),

suggested that GEN was leaving only a few unreacted lysine residues free in the WG for the EDTAD acylation. On the other hand, the increase in swelling by adding 4 wt% GEN, as compared to WG, is due to the high polarity of the reacted GEN molecule after the alkaline/thermal treatment (forming two aldehydes on its monomeric form and a charged carboxylic acid group by the hydrolysis of the methyl ester group, see Section 2.3).<sup>[27]</sup> The hydrolysis of the GEN methyl ester pendant group, forming a charged carboxylic acid group, leads to the higher water uptake of the WG samples containing GEN, even in the absence of EDTAD.<sup>[36,37]</sup>

The centrifugation test (CRC) of the WG25ED4GEN revealed that  $\approx 80\%$  of the water was held strongly in the protein hydrogel (Table 1). This represents  $\approx 13$  and 4 times increase in the CRC compared to the pristine WG and WG4GEN25ED, respectively. This shows the strong synergy effects obtained by first acylating the WG protein with EDTAD and subsequently cross-linking it with GEN. The most representative WG-based hydrogels after 24 h swelling and the centrifuged materials after 30 min swelling (both in water) are displayed and compared with commercial synthetic SAPs materials in Video S1 and Video S2, Supporting Information, respectively.

The saline uptake in WG25ED4GEN was  $\approx 5.5 \text{ g g}^{-1}$  (30 min) and  $\approx 4.8 \text{ g g}^{-1}$  (24 h) (Figure 1b). The depletion was a consequence of the loss of material after longer periods in saline and some deswelling occurring at longer times, as also observed for synthetic SAP materials when swollen in saline solution. The overall decrease in the swelling in saline, in contrast to water, is a consequence of lower osmotic pressure and repulsion in the treated chains due to the sodium ions present in the liquid.<sup>[38,39]</sup> Nonetheless, the saline swelling of WG25ED4GEN increased by  $\approx 4$  and 2 times compared to WG and WG4GEN25ED, respectively. The 30 min saline CRC indicated retention of  $\approx 48\%$  of the liquid (Table 1), which is comparable to that of synthetic SAP tested in saline ( $\approx 66\%$ ). This, again, indicates that the addition of GEN after the EDTAD acylation is important for obtaining high swelling and retention values. The defibrinated sheep blood absorption in WG25ED4GEN after 30 min was  $2.3 \text{ g g}^{-1}$ , which was 50% higher than the as-received WG ( $1.55 \text{ g g}^{-1}$ ). Moreover, the CRC of WG25ED4GEN in sheep blood was  $2.8 \text{ g g}^{-1}$ , which represents 25% of the CRC for

commercial highly charged SAP particles encountered in daily-care products ( $11.2 \text{ g g}^{-1}$ ).

When GEN was instead added before the acylation (WG4GEN25ED), the material was only able to swell  $\approx 3.5 \text{ g g}^{-1}$  in saline (24 h) (Figure 1b). This sample also showed a more intense blue color compared to when GEN was added after the acylation (WG25ED4GEN). The origin of the blue color has been acknowledged to the oxygen radical-induced polymerization/complexation of GEN during the cross-linking of the lysine moiety in the protein (Figure 1c-4 and Figure 2).<sup>[30,35]</sup> The suggested acylation scheme between WG and EDTAD (WG25ED), cross-linking of the WG with GEN (WG4GEN) and cross-linking of the acylated-WG protein (WG25ED4GEN) is shown in Figure 3. The EDTAD and GEN have been previously reported as mainly reacting through the condensation of the reagent with the lysine residues of the protein, forming an amide bond and imide bond, respectively (Figure 3a,b).<sup>[3,4,17]</sup> The bifunctional and complex structure of GEN (Figure 3b) results in cross-linking mechanisms that are complex but of interest for the development of nonharmful sustainable materials.<sup>[40]</sup> GEN can also, e.g., undergo self-polymerization due to ring-opening reactions via nucleophilic attack, hydrolysis of the methyl-ester group, etc.<sup>[41,42]</sup> Other reported reactions that are likely involved between other amino acid residues in the WG in alkali conditions and/or involving EDTAD, e.g. tyrosine cross-linking and deamination of glutamine/asparagine,<sup>[43,44]</sup> are not illustrated in Figure 3.

## 2.2. Protein Polymerization

Acylation of the WG increased the amount of protein extracted through the cleavage of secondary bonds (WG versus WG25ED, Ext. 1). Furthermore, the total amount of extracted protein increased, indicating a less stable network/more soluble material after acylation (Figure 4a). Besides, most of the protein extraction from WG25ED occurred in Ext. 1 and Ext. 2 (total  $\approx 100\%$ ), whereas, for WG and WGRef sizeable extraction still occurred in Ext. 3 as they were not depleted by earlier extractions (Figure 4a). The solubility of the polymeric protein fraction ( $\approx 10$  min elution time, Ext. 1, Figure S1, Supporting Information) increased substantially in WG25ED (60%) in comparison with WG (47%) (Figure 4b), in accordance with the network instability of this sample during the swelling test (Figure 1a). The reduction in protein extractability from WGRef, compared to the pristine powder (WG) (Figure 4a and S1, Supporting Information), is most likely due to protein cross-linking as a consequence of the alkali treatment and acid precipitation leading to a different UV absorbance.<sup>[45,46]</sup> In addition, proteins with a low level of protein–protein interaction remained in the supernatant (SN) of WGRef after the alkali treatment and acid precipitation (during the sample preparation), leading to the yield reduction for WGRef (Table 2). The removal of the proteins with a low level of protein–protein interaction also contributes to the low extractability in WGRef Ext.1 as compared to WG and also impacts the total protein extractability (Figure 4b). The decrease in the absorbance at the highest wavelength tested here (220 nm, Figure S1, Supporting Information) and the shift of the value of the peak maxima in WGRef (at 15.4 min, Figure S1

**Table 1.** Centrifuge retention capacity (CRC) values for the different samples.

Sample	Liquid	CRC [g/g]
WG	Saline	$1.52 \pm 0.02$
WGRef	Water	$1.17 \pm 0.10$
	Saline	$1.37 \pm 0.07$
WG25ED	Water	Not possible
	Saline	$2.72 \pm 0.04$
WG4GEN	Saline	$1.46 \pm 0.05$
WG25ED4GEN	Water	$20.49 \pm 0.10$
	Saline	$2.62 \pm 0.20$
WG4GEN25ED	Water	$4.92 \pm 0.20$
	Saline	$1.53 \pm 0.03$

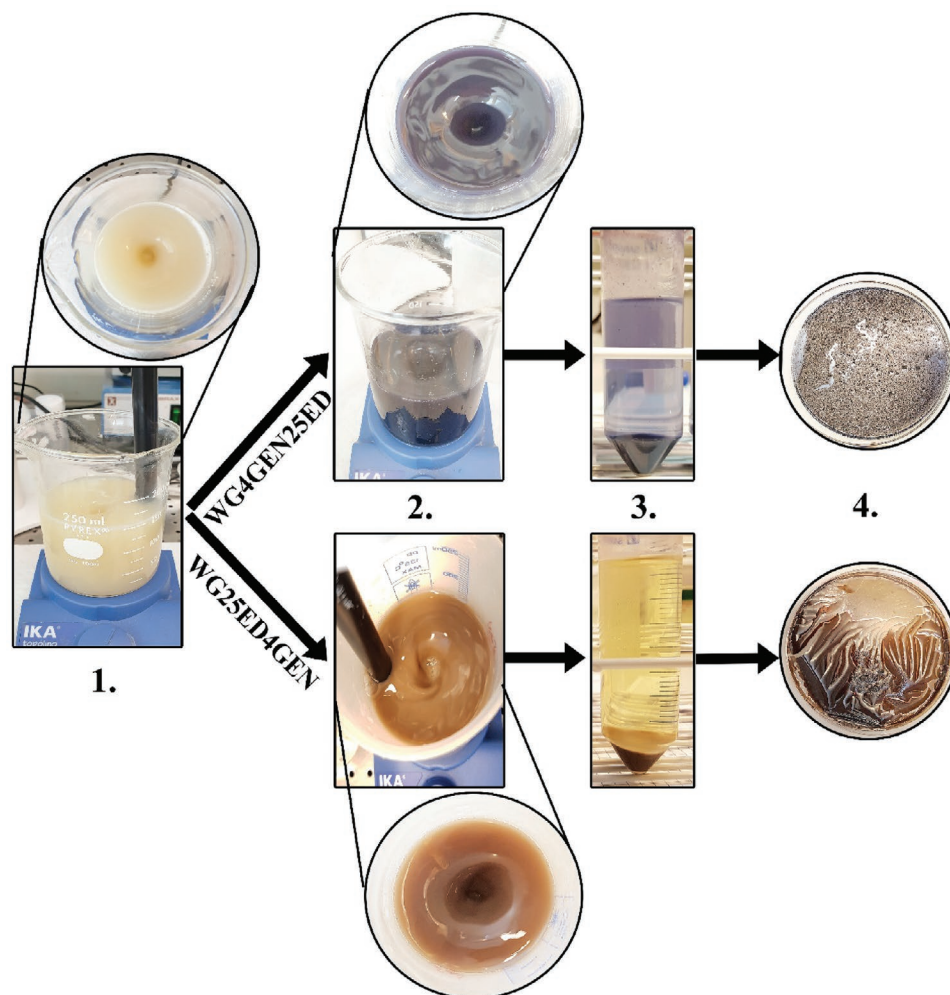


**Figure 2.** Images illustrating the different reaction steps for WG4GEN25ED and WG25ED4GEN. (1) 2 wt% WG suspension, (2) the reacted mixture after the GEN/EDTAD (upper images) and EDTAD/GEN reactions (lower images) reactions, (3) pellets and SN after centrifugation, and (4) films after drying.

(Supporting Information) WGR<sub>ef</sub> b,c) might indicate tyrosine reactions in the WG, which has been suggested previously as a cross-linking reaction.<sup>[43,44,47]</sup> Similar peak maxima value and decrease in absorbance at the highest wavelength were found for the WG25ED as described for WG (Figure S1b,c, Supporting Information), indicating a lack of cross-linking and higher protein solubility by the addition of only EDTAD. However, all samples containing GEN (WG25ED4GEN, WG4GEN, and WG4GEN25ED), showed a lower peak maxima value at 15.4 min and almost no decrease in absorbance at the highest wavelength, similarly as described above for WGR<sub>ef</sub>, which suggests that GEN reacts with the aromatic residues of the WG protein (Figure S1, Supporting Information).

The use of only 4 wt% GEN in WG (WG4GEN) demonstrates its important cross-linking effect on the protein (Figure 4). High sonication energy/long time applied in extractions 2 (Ext. 2) and 3 (Ext. 3) were used to disrupt S–S cross-links in the WG4GEN and still only ≈50% of the protein was extracted compared to WG (Figure 4a and Figure S1, Supporting Information). This, coupled with the fact that the

extracted proteins in WG4GEN consisted of 70% of PP fractions (Figure 4b), reveals the strong cross-linked WG network of WG4GEN and correlates with the low swelling of this sample (Figure 1). The PP/MP ratio (55/45%, Figure 4b) and strong sonication treatment needed to solubilize the protein (40% Ext. 3) in WG25ED4GEN compared to WG25ED (70% Ext. 1), showed that the 4 wt% GEN addition after the EDTAD acylation was sufficient to provide a network of acylated WG. The change in color of WG25ED4GEN to brownish indicated that the GEN did react with unreacted lysine and/or other residues, e.g., tyrosine after the EDTAD treatment. However, the lighter color of WG25ED4GEN compared to WG4GEN (Figures 1 and 2), agrees with previous studies indicating a lower degree of GEN cross-linking and GEN self-polymerization reactions,<sup>[48]</sup> which in parallel contribute to the super swelling properties of WG25ED4GEN.

When the GEN was added before acylation (WG4GEN25ED), the protein extraction profiles resembled that of WG4GEN (Figure 4a, Ext. 1 and 2), although with a reduced amount of protein being extracted in Ext. 3 than for WG4GEN (Figure 4a),

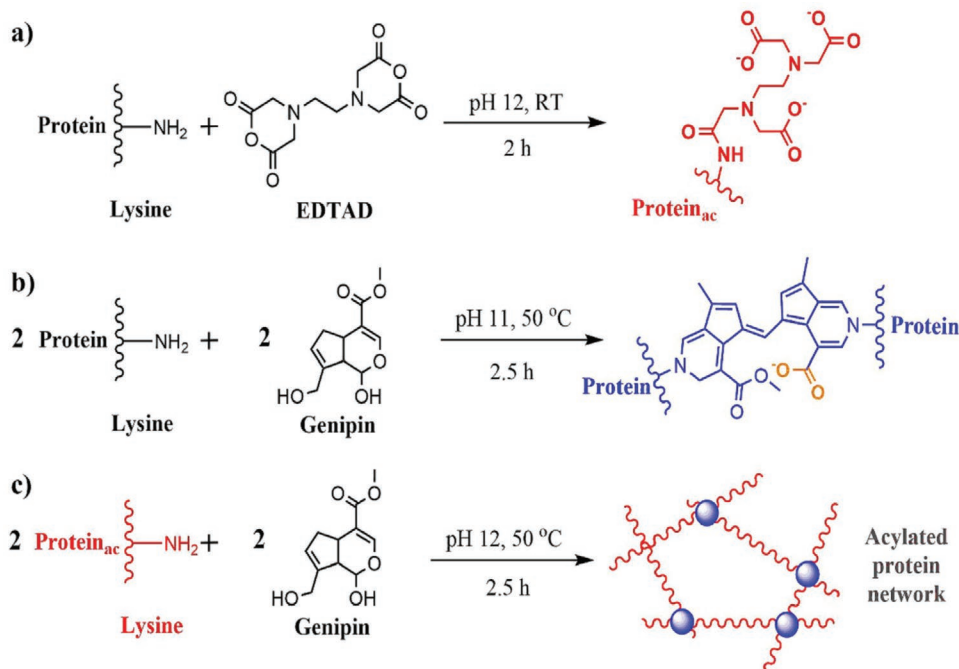


Figure 3. Schemes of the protein acylation using EDTAD (a), protein cross-linking using GEN (b) and cross-linking of acylated proteins with GEN (c).

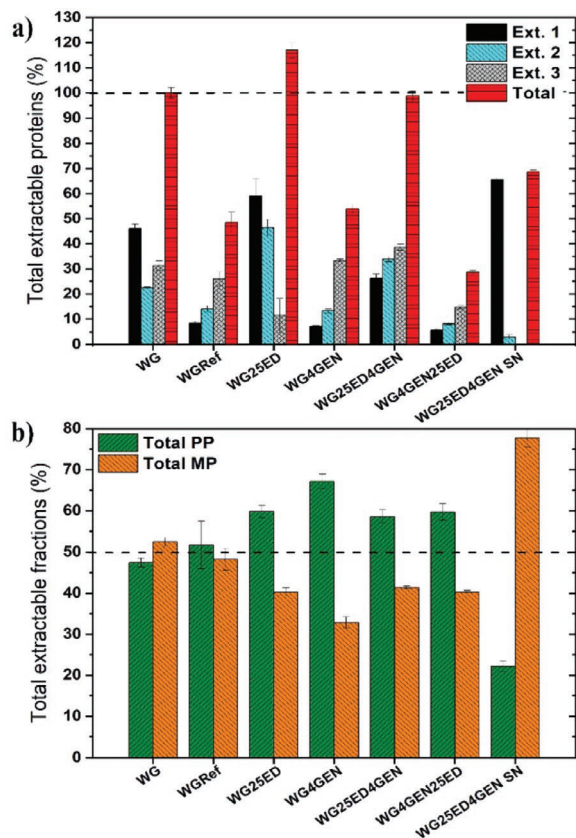


Figure 4. Total extractable proteins obtained by SE-HPLC (a) and the polymeric (PP) and monomeric (MP) extractable fractions (b). The total amount of extractable proteins in the WG sample was used as a normalized reference value for the other samples.

indicating increased cross-linking for the WG4GEN25GEN. Previous studies have primarily used EDTAD for protein acylation/carboxylation in dilute protein solutions with an excess of EDTAD to avoid cross-linking of the protein by the dianhydride.<sup>[3,4,17]</sup> Therefore, the pre cross-links generated by the GEN in WG4GEN25ED seemed to favor additional cross-links by the EDTAD, thus explaining the lower extractability in that sample compared to WG4GEN (Figure 4a). These results agree with the swelling results (Figure 1). The size-exclusion high-performance liquid chromatography (SE-HPLC) analysis on the supernatant (SN) coming from the cleaning of the product WG25ED4GEN after the acid precipitation (WG25ED4GEN SN) demonstrated that it mainly consisted of low molecular weight peptides (MP, Figure 4b) further indicating a well-developed network.

### 2.3. Chemical Characterization

The  $1525\text{ cm}^{-1}$  peak in the amide II region (C=O stretching and N-H bending) was more prominent in all the acylated samples than in WG and WGRef, which indicated a larger content of amide bonds in these samples (Figure 5a,b).<sup>[49]</sup> This is due to the acylation reaction between EDTAD and the lysine residue, forming amide bonds (Figure 3). In addition, the increase in the peak intensity for the amide II region ( $1550\text{--}1500\text{ cm}^{-1}$ ) has been ascribed to an increase in hydrogen bonding in proteins.<sup>[50]</sup> The shoulder observed in the region  $1432\text{--}1422$  and the peak at  $1395\text{ cm}^{-1}$  for WG25ED, WG25ED4GEN, and WG4GEN25ED (Figure 5c) indicate the presence of pendant carboxylic acid groups (symmetric stretching of the  $\text{--OH}$ ). Symmetric stretching of charged carboxylic acid groups

**Table 2.** Sample description.

Sample <sup>a)</sup>	WG [%]	EDTAD [%]	GEN [%]	Yield [%] <sup>b)</sup>	Protein <sup>c)</sup> [%]
WG	100			N/A	84.8 ± 0.4
WGRef	100			82.5	84.5 ± 0.5
WG25ED	80	20		65.0	89.7 ± 0.5
WG4GEN	96.2		3.85	75.9	
WG25ED4GEN	77.5	19.4	3.10	71.8	81.4 ± 0.6
WG4GEN25ED	77.5	19.4	3.10	70.8	86.4 ± 0.1

<sup>a)</sup>(% refer to weight); <sup>b)</sup>(The dried films were weighed after removal from the oven and the weight was compared to the total initial mass added to each recipe); <sup>c)</sup>(Using the Dumas method and 6.25 as the conversion factor)

neutralized with Na<sup>+</sup> ions has been ascribed to 1432 cm<sup>-1</sup>.<sup>[51,52]</sup> These results agree with the acylation scheme shown in Figure 3. The increase of the peak intensity at 1078 cm<sup>-1</sup> (here observed for WG4GEN) has been explained by the formation of C–O and/or C–N bonds (stretching motions) when the heterocyclic complex of GEN has been formed during the cross-linking of the protein (Figures 3b and 5a).<sup>[30,53]</sup> The decrease in this peak for WG25ED4GEN indicates less cross-linking with GEN, which is following with the high water uptake obtained for this sample compared to WG4GEN (Figure 1).

To evaluate the structural evolution of the individual reagents in the acylation conditions used, EDTAD was reacted under alkali conditions alone (rxEDTAD), simulating the reaction conditions used to acylate the WG protein (WG25ED process). The absence of the characteristic peaks for EDTAD (1805 and 1749 cm<sup>-1</sup>) in all the acylated protein samples indicates that the excess EDTAD has been removed from the materials (compare Figure S2a (Supporting Information) and Figure 5). The absence of the peaks at 849 and 710 cm<sup>-1</sup> in the acylated samples (Figure 5), corresponding to free reacted EDTAD (Figure S2a, Supporting Information), suggests that the nongrafted reacted EDTAD has been removed from the protein sample. However, as the acylated samples also contain grafted EDTAD molecules

having similar vibration bands, the conclusion cannot be fully supported. Nonetheless, traces of reacted EDTAD in the superabsorbent particles are not considered harmful for an industrial product.<sup>[54]</sup>

The <sup>1</sup>H NMR spectra for rxEDTAD showed a shift in the protons as compared to the EDTAD spectrum (Figure 6a,c). The EDTAD (DMSO-*d*<sub>6</sub>, 400 MHz) had a shift corresponding to δ 2.67 (s, 4H, N(CH<sub>2</sub>)<sub>2</sub>N), and 3.71 (s, 8H, O=CCH<sub>2</sub>N). As shown in Figure 6a, the rxEDTAD (D<sub>2</sub>O, 400 MHz) appears with two single peaks at δ 3.05 ppm corresponding to the eight methylene protons of acetyl moieties, and at δ 2.50 ppm corresponding to the four protons of the ethylenediamine moiety. This corresponds to the ring-opening reaction of the EDTAD in the alkali aqueous solution forming four charged-carboxylic acid groups. The absence of other shifts in the rxEDTAD, coupled with its total solubility in deuterium oxide, indicates the presence of carboxylate pendant groups and not carboxylic acids. The NMR result agrees with the Fourier transform infrared spectroscopy (FTIR) of the rxEDTAD (Figure S2a, Supporting Information), confirming the formation of charged-carboxylic acid groups, i.e., with the presence of the peaks at 1595 and 1401 cm<sup>-1</sup> (–COO<sup>-</sup> asymmetric and symmetric stretching, respectively)<sup>[52,55]</sup> and 1325 cm<sup>-1</sup> (–CH<sub>2</sub>(COO<sup>-</sup>) tetrasodium EDTA).<sup>[52,56]</sup> The HPLC/MS profile in Figure S3a (Supporting Information) for the rxEDTAD further confirmed the formation of charged EDTA under the actual reaction conditions, agreeing with the FTIR and NMR results (Figures S2a and 6a, Supporting Information, respectively). The matrix-assisted laser desorption ionization-time of flight (MALDI-TOF) data shown in Figure S4a (Supporting Information) suggests that the rxEDTAD could also form dimers and trimers by the formation of an amide link between reacted EDTAD and unreacted EDTAD.

The structural changes on GEN were also studied by reacting solely the GEN in alkali (pH 12) solution and elevated temperature (50 °C), simulating the reaction conditions for the preparation of WG4GEN (rxGEN). A change in color of the

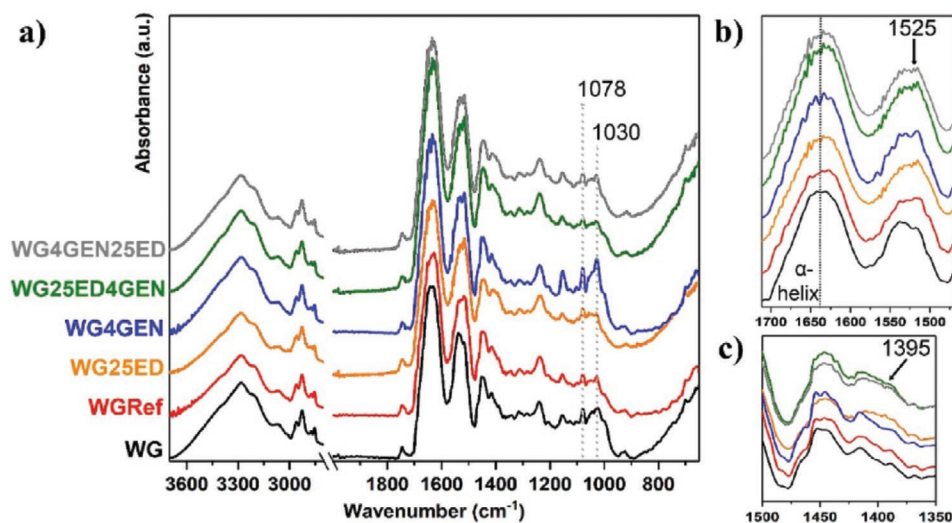


**Figure 5.** Fourier transform infrared spectroscopy (FTIR) data for the different samples (a) and a close-up of the amide I and II region (b) and the 1500–1350 cm<sup>-1</sup> region (c).

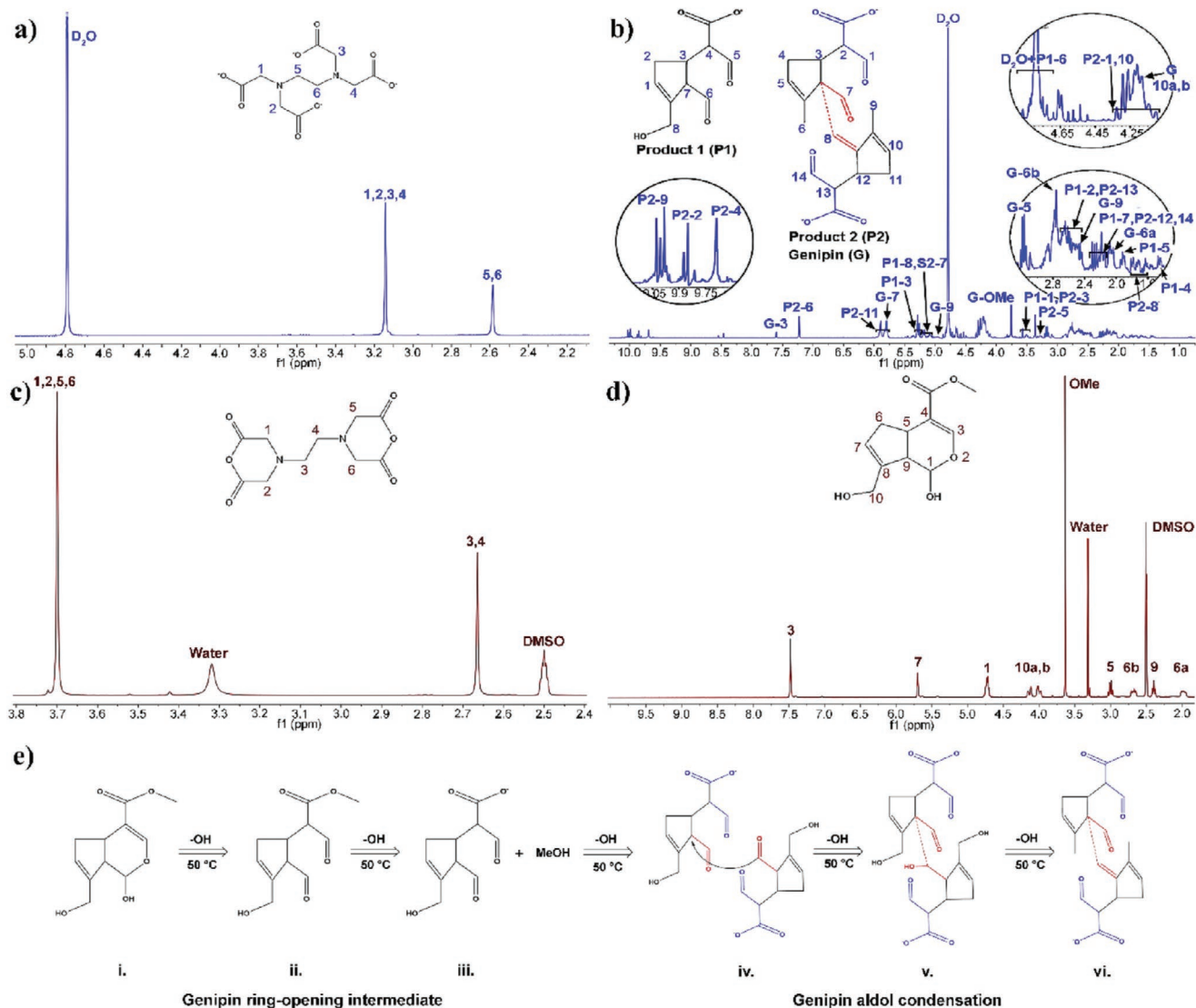


**Figure 6.**  $^1\text{H}$  NMR of the rxEDTAD (a), rxGEN (b), ethylenediaminetetraacetic (EDTAD) (c), and GEN (d).

solution from colorless to brownish occurred within the first 30 min of reaction (Figure S2b, inset, Supporting Information). The reaction of GEN (rxGEN) resulted in FTIR bands at, e.g., 1714, 1590, 1400, and 1348  $\text{cm}^{-1}$  (Figure S2b, Supporting Information). The bands at 2990–2850 and 1714  $\text{cm}^{-1}$  in the rxGEN spectrum are assigned to the stretching of  $-\text{C}-\text{H}$  and  $-\text{C}=\text{O}$  of an aldehyde functionality.<sup>[57,58]</sup> The peaks at 1590 and 1400  $\text{cm}^{-1}$ , together with the peak at 1348  $\text{cm}^{-1}$ , in the rxGEN are due to the formation of charged-carboxylic acid groups.<sup>[52,56]</sup> The formation of  $-\text{COO}^-$  on the GEN molecule after the alkali/thermal treatment is suggested to come from the hydrolysis of the methyl ester bond in the GEN.<sup>[48,51,52]</sup> The obtained  $^1\text{H}$  NMR spectrum from the rxGEN is shown in Figure 6b, showing that rxGEN is a complex mixture of different products. The different suggested products contained in rxGEN were also analyzed using 2D  $^1\text{H}$  COSY NMR (Figure S5, Supporting Information). The Product 1 (P1) unit (Figure 6b) is confirmed by the strong signal of peaks in the region  $\delta$  5.20 (1H, t,  $J$  = 8 Hz, H-3),

5.16–4.94 (2H, H-8), 4.79–4.60 (1H, H-6), 3.50–3.36 (1H, H-1), 2.62–2.39 (2H, H-2), 2.24–2.03 (1H, H-7), 1.87–1.74 (1H, m, H-5), and 1.41–1.26 (1H, m, H-4). The GEN  $^1\text{H}$  NMR (DMSO- $d_6$ , 400 MHz) spectrum contains:  $\delta$  1.99 (1H, br dddd, H-6a), 2.40 (1H, t,  $J$  = 8 Hz, H-9), 2.68 (1H, br-dd, H-6b), 3.01 (1H, q,  $J$  = 8 Hz, H-5), 3.64 (3H, s, OMe), 4.01, 4.15 (each 1H, d,  $J$  = 12 Hz, H-10), 4.75 (1H, q,  $J$  = 12 Hz, H-1), 5.71 (1H, s, H-7), and 7.48 (1H, s, H-3) (Figure 6d). Likewise, the other signals obtained in Figure 6b are attributed to the structure of unreacted GEN (G) and Product 2 (P2). The peaks for Product 2 are:  $\delta$  10.01–9.86 (3H, m, H-9), 9.76 (1H, t,  $J$  = 16 Hz, H-2), 9.60 (2H, t,  $J$  = 4 Hz, H-4), 7.14 (3H, s, H-6), 5.93–5.66 (2H, H-11), 5.16–4.94 (1H, H-7), 4.26–3.98 (1H+1H, H-1, H-10), 3.50–3.36 (1H, H-3), 3.25–3.14 (1H, m, H-5), 2.62–2.39 (1H, H-13), 2.24–2.03 (1H+1H, H-12, H-14), and 1.73–2.51 (1H, m, H-8).

The complex mixture of P1, P2, and unreacted genipin structures, in addition to possible further degradation products of GEN in the rxGEN solution, was also confirmed by the

molecular weight profile (Figure S4b, Supporting Information). A suggested reaction scheme of the complex mixture in the rxGEN is shown in Figure 6e. The ring-opening reaction of GEN under alkaline condition has been previously reported, where two aldehyde groups (di-hydrated) are formed as the precursor for further reactions (Figure 6eii).<sup>[59,60]</sup> Alkaline conditions at elevated temperature (here 50 °C) have also been reported to hydrolyze the methyl ester group in the GEN, in agreement with the FTIR, mass spectrometry (MS), and <sup>1</sup>H NMR results here (Figure 6eiii).<sup>[48]</sup> In the present alkaline conditions, the unstable molecule (iii) undergoes self-polymerization via aldol condensation of the aldehyde moieties between two GEN molecules (Figure 6eiv-v). Finally, the present conditions further dehydrate the dimer product leading to the formation of an alkane bond and methyl groups.<sup>[35,61]</sup> The broad band at 3300-3000 cm<sup>-1</sup> observed in rxGEN (Figure S2b, Supporting Information) is assigned to -OH interaction coming from P1 (Figure 6eiii). The presence of P2 in rxGEN (Figure 6evi) was also confirmed by the peaks occurring at 1550 cm<sup>-1</sup> and 2900 cm<sup>-1</sup> (C=C and C-H stretching of the alkene and methyl group) and 930 cm<sup>-1</sup> (C-H bending of the alkene),<sup>[30,48,62]</sup> formed as a consequence of the aldol condensation reaction (Figure S2b, Supporting Information). Although previous studies have shown that GEN (reacted with chitosan) can undergo self-polymerization, only oligomers based on trimers of GEN were observed in Figure S4b (Supporting Information), which is suggested to be a consequence of the shorter reaction time (here 2 h) of the rxGEN as compared to the previous studies (>5 h reaction time).<sup>[32,48,63]</sup>

GEN was also added to a rxEDTAD solution to simulate the reaction conditions in WG25ED4GEN, between EDTAD and GEN (rxEDTAD/GEN). The rxEDTAD/GEN solution turned brownish after 30 min of the GEN addition, having a similar color to the rxGEN solution without EDTAD (Figure S6, Supporting Information). The HPLC/MS of the rxEDTAD/GEN data shows that the mixture between reacted EDTAD and GEN did not effect on the retention time for the rxEDTAD nor in their molecular weight (Figure S3a,c, Supporting Information). The FTIR of the rxEDTAD/GEN (Figure S7a, Supporting Information) showed a similar profile as for the rxEDTAD (Figure 5), with a sharp peak at 881 cm<sup>-1</sup> (C-H bending of the alkene from the rxGEN), suggesting no evident reaction between the two reagents. The other bands corresponding to rxGEN in rxEDTAD/GEN are overlapped by the strong signals from rxEDTAD, which accounts for ≈86% of the dry weight in the rxEDTAD/GEN powder. In addition, the <sup>1</sup>H NMR performed on rxEDTAD/GEN (D<sub>2</sub>O, 400 MHz) (Figure S7b, Supporting Information) showed no moderate shifts in the characteristic peaks for rxEDTAD (Figure 6a), while the weak peaks from the rxGEN are observed (Figure 6b).

The results suggest that in the presence of the protein, GEN reacts with the lysine residues remaining after the EDTAD-acylation (Figure 3c), rather than GEN reacting on the EDTAD-grafted molecules on the protein. The reaction of GEN will then provide sufficient cross-links in the protein (by the reaction of two GEN molecules, Figure 3b), allowing the protein network to form a stable hydrogel after swelling in water (Figure 1a). The results also suggest that the highly reactive double aldehyde GEN intermediate formed (shown in rxGEN, Figure 6eiii)

can also react with other WG protein residues containing α-amino groups, e.g. arginine and glutamine, grafting the polar rxGEN onto the protein and contributing further to the high swelling degree of the material. The grafting of the polar rxGEN, adding additional charged carboxylic acid groups to the protein, in combination with the rxEDTAD, thereby promotes a WG network with higher electrostatic repulsion/osmotic contribution leading to the rapid and higher liquid retention properties in WG25ED4GEN (Figure 1 and Table 1). Finally, the evidence of the separate condensation of EDTAD and GEN molecules, forming separately charged carboxylate oligomers (rxGEN and rxEDTAD), paves the way for future optimization work, e.g., the formation of interpenetrated networks between protein, EDTAD, and GEN for the future sustainable superabsorbent material. The combined high swelling and super liquid retention of WG25ED4GEN, together with the super biodegradability reported for GEN-cross-linked protein materials (≈19 days after burial),<sup>[64]</sup> provides the frame to produce safe disposable SAP products that can contribute within the cradle-to-cradle approach for producing sustainable materials,<sup>[40]</sup> which is necessary to fully compete with the synthetic SAP counterparts.

#### 2.4. Particles Thermal Stability and Morphology

Thermogravimetric analysis revealed that the maximum mass loss rate of WGRef, WG4GEN, and WG4GEN25ED occurred at ≈325 °C, which was higher than for WG (309 °C, Figure 7, inset). This increase in thermal stability in the gluten protein isolate has been previously reported as an indication of an increase in the degree of protein cross-linking.<sup>[65]</sup> The lowest temperature of maximum mass loss rate was observed for WG25ED4GEN (at ≈302 °C), which agree with previous results reported on carboxylated WG<sup>[24,66]</sup> suggests lower thermal

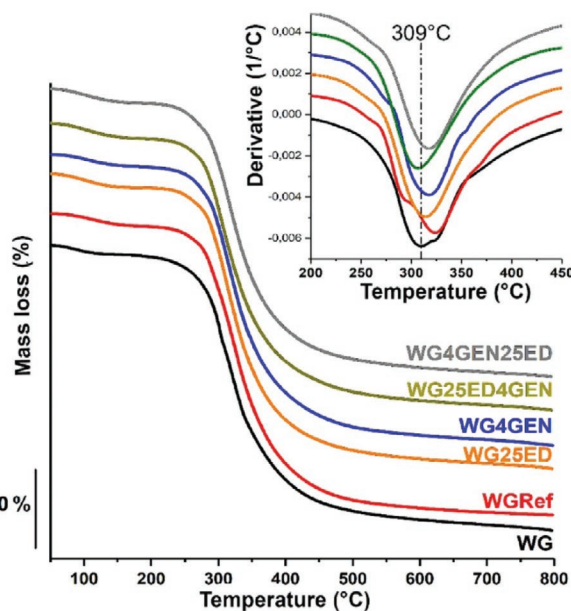


**Figure 7.** TGA profiles of the different samples. The inset shows the first derivative of the mass versus temperature curve. Curves have been stacked vertically for clarity.

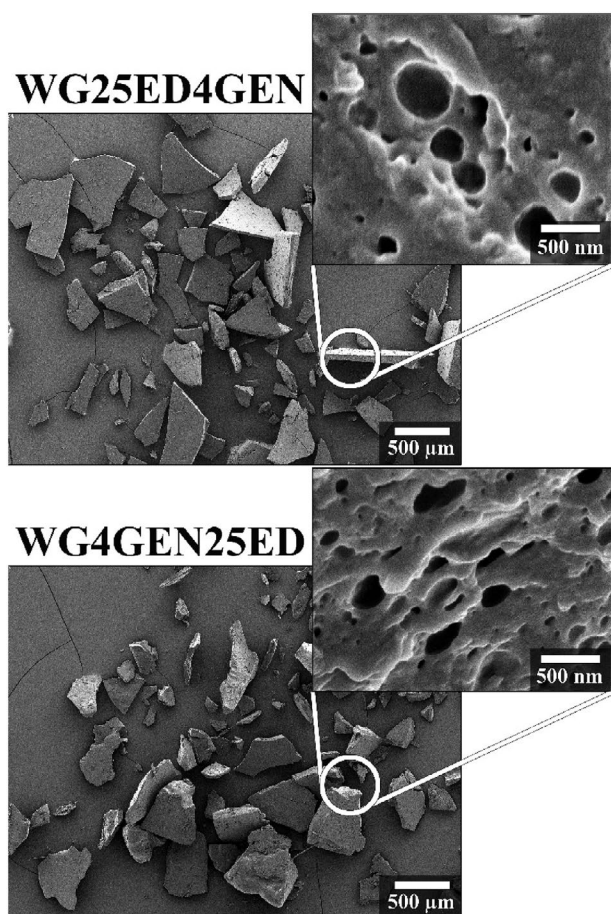


**Figure 8.** Scanning electron microscope (SEM) images of the dry particles.

stability due to the carboxylate groups added during the EDTAD treatment.

The particle size of WG25ED4GEN and WG4GEN25ED were  $340 \pm 195$  and  $267 \pm 155$   $\mu\text{m}$ , respectively (Figure 8). This is within the range of commercial SAP particles (150–350  $\mu\text{m}$ ).<sup>[11]</sup> Nano-sized pores with  $\approx 300$  nm in diameter were observed in these samples, which are suggested to develop during the drying process of the materials (Figure 8, inset).<sup>[26]</sup> These pores are beneficial for daily-care products since they are expected to contribute to a faster liquid uptake by capillary action,<sup>[1,11,27]</sup> as observed here with  $\approx 7$  g g<sup>-1</sup> of water swelling in less than 1 min (Figure 1a). The particle morphology and the readily obtained porosity, having the capacity of providing a rapid initial swelling and improved liquid distribution, paves the way for the future re-design of daily-care products and promotion for more detailed studies regarding the specific swelling characteristics of the material in different sanitary products.

WG25ED4GEN was immersed in water (24 h), frozen, and lyophilized. The particle shape of the original material (Figure 8) was lost during 24 h immersion in water as individual particles were not visible after lyophilization (Figure 9). Instead, a foam structure with large interconnected pores was formed due to the large water content of the swollen WG25ED4GEN and subsequent ice crystal formation and sublimation during

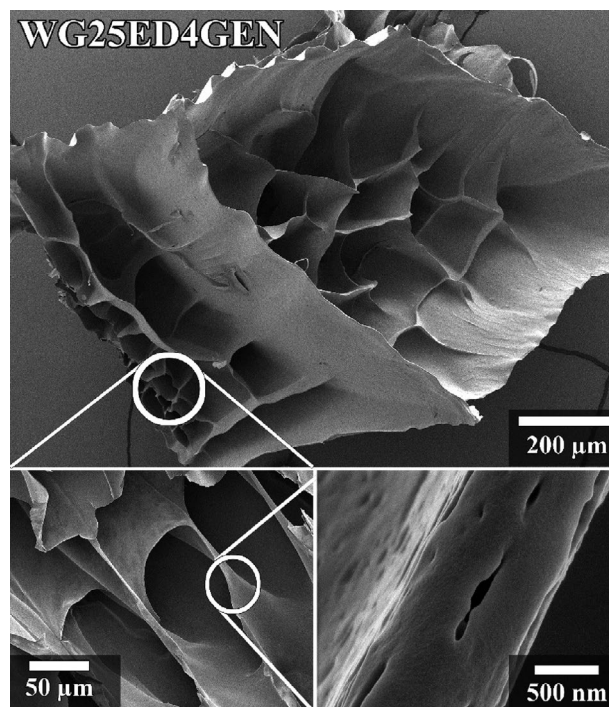


**Figure 9.** Micrographs of the lyophilized WG25ED4GEN material after 24 h immersion in water (the tea-bag test).

the freeze-drying process. The thickness of the formed cell walls was 500–600 nm. The shape of the foams after swelling indicates that the individual WG25ED4GEN particles fused forming the swollen hydrogels observed in Video S1 (Supporting Information, Figure 9). This type of “water-welding”/fusion has been previously reported for WG foams when placed in direct contact with liquid water.<sup>[67]</sup>

A foam structure was also observed for the WG4GEN25ED sample (Figure 10a), with particle fragments of  $\approx 500$   $\mu\text{m}$  in size with a  $30 \pm 10$   $\mu\text{m}$  pore diameter. In addition, the lyophilization of the WG4GEN25ED sample swollen in saline during 24 h revealed evenly distributed NaCl crystals embedded in the cell walls (Figure 10b). This verified that the liquid had fully penetrated the solid WG particles, as also demonstrated by the high liquid retention capacity of these materials (Table 1).

### 3. Conclusion

The addition of a nontoxic natural cross-linker (GEN) to WG not only provided a stable network of acylated protein material but also resulted in a flexible superabsorbent showing synergistic effects simultaneously displaying high water swelling and holding capacity. The absorbent showed water and saline swelling of  $\approx 40$  and  $6$  g g<sup>-1</sup>, respectively, i.e., 4000 and 600% weight increase. The material was also able to retain  $\approx 80\%$  and 50% of the liquids within the hydrogel after centrifugation, representing values similar to those that can be found in commercial fossil-based superabsorbents. The presented lysine-acylation of the WG molecular chains is particularly effective and useful for functionalizing protein molecules containing

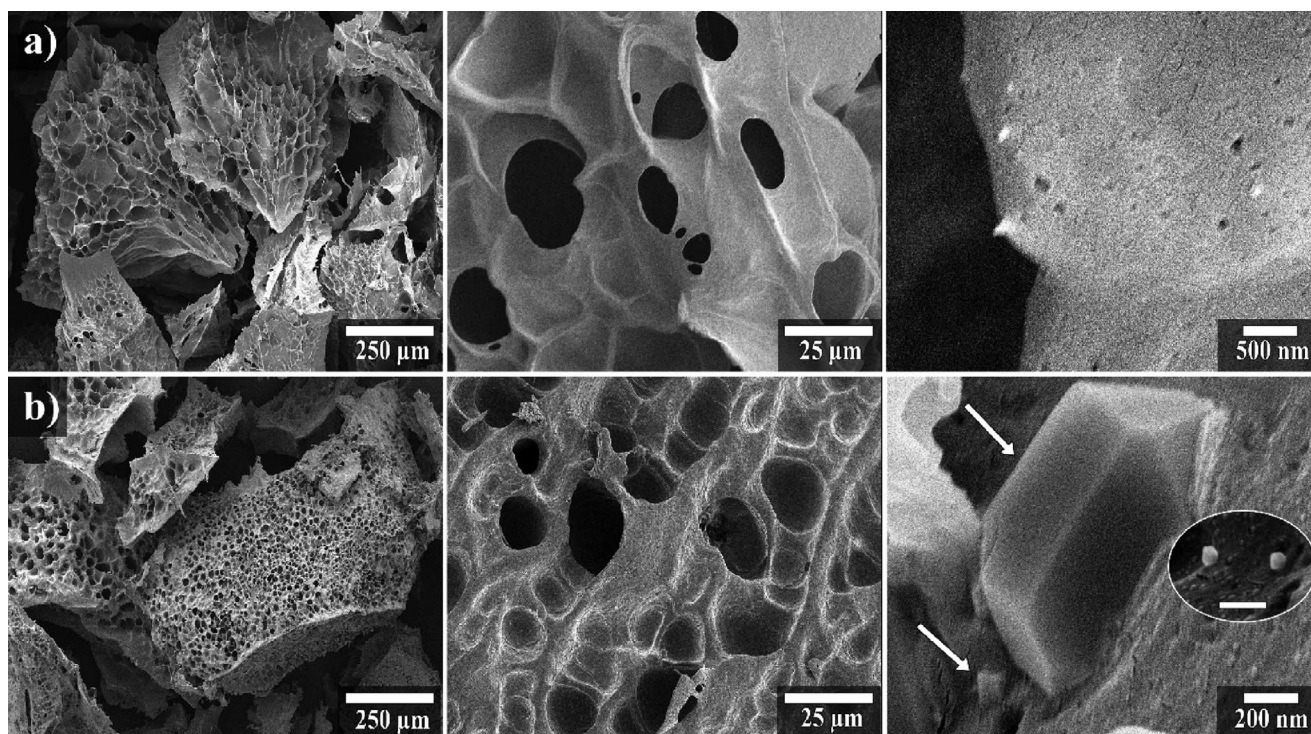


**Figure 10.** The lyophilized WG4GEN25ED particles after 24 h immersion in water (a) and saline (b). Arrows point at salt crystals. The scale bar in the inset is 200 nm.

low amounts of lysine residues. Considering that the current SAP products do not follow the general environmental channels of traditional polyolefin plastics that require reduce, reuse, and recycling strategies, the implementation of cradle-to-cradle approaches is of particular importance among the daily-care products since they rely on being disposable. The unique viscoelastic nature of the cross-linked gluten polymeric materials prepared from renewable resources herein presented allows for the first time envisioning large-scale production of environment-friendly SAP materials. The functional rich protein molecules provide many opportunities for additional modifications and cross-linking reactions, opening-up for additional new material applications. It is foreseen that the illustrated concept of the enclosed protein material development inspires toward a wider expansion among the UN sustainable development goals, in addition to the already targeted sustainable cities and responsible consumption goals (11 and 12).<sup>[68]</sup>

#### 4. Experimental Section

**Materials:** WG was provided by Lantmännen Reppe AB, Sweden. The reported protein content of the as-received WG powder was  $86.3 \pm 0.3$  wt%, with a moisture content of  $6.6 \pm 0.6$  wt%. The fat and ash contents were  $0.9 \pm 0.1$  and  $0.8 \pm 0.1$  wt%, respectively (2009/152/EU mod and NMKL 173). EDTAD (98%), acetonitrile 99.8%, 2,5-dihydroxybenzoic acid (DHB) (HPLC grade), sodium dodecyl sulphate (SDS) (ACS grade), sodium phosphate monobasic ( $\text{NaH}_2\text{PO}_4$ ) (HPLC grade), were purchased from Sigma-Aldrich, Sweden. GEN  $\geq 98\%$  (HPLC grade) was purchased from Zhixin Biotechnology, China. The defibrinated sheep blood was obtained from the Disease Vector Group, Swedish University of Agricultural Sciences, Sweden. The nitrogen content of all the materials prepared was obtained by the Dumas method using a Flash 2000 NC

Analyzer (Thermo Scientific, USA), in triplicate. The nitrogen-to-protein conversion factor used was 6.25.

**Synthesis of WG25ED:** The as-received WG powder was acylated as previously described by Damodaran and Cuadri et al.<sup>[3,13]</sup> with some modifications. A suspension of Millipore water (MQw) pre-adjusted to pH 11 (using 1 M NaOH) and 2 wt% WG powder was prepared in a beaker. The WG powder was gradually added to the beaker under constant stirring (Figure 2-1). For denaturing the protein and to expose the native functional groups of the WG, the suspension was placed in a preheated water bath at  $90 \pm 2$  °C and stirred 30 min.<sup>[22,23,69]</sup> Thereafter, the suspension was cooled to room temperature (RT) with an ice-bath. For the acylation, the pH of the WG suspension was raised to 12 and gradual amounts of EDTAD were added to the denatured WG over 30 min until reaching 25 wt% EDTAD relative to the WG content (i.e., 25/100 w/w). The pH of the suspensions was monitored using a SevenCompact pH/ion pH-meter (Mettler Toledo, USA) and adjusted to 12 using 1 M NaOH. The acylation proceeded during 1.5 h. For cleaning the acylated-WG from unreacted EDTAD salts, the pH of the suspension was adjusted to 3 (1 M HCl) to precipitate the WG. Then, the suspension was centrifuged at 3900 RCF, 5 min, using a Sorvall RC6+ Centrifuge (Thermo Scientific, USA). The SN was replaced by fresh MQw, the pH adjusted to 3, and the pellet was shaken at 2000 rpm for 5 min and centrifuged as in the previous step. The pellet was redispersed in MQw to 25% of the initial volume and the pH was adjusted to near neutral conditions ( $\approx 7.5$ -8) using 1 M NaOH. The acylated-WG was poured into a petri-dish and dried overnight at 40 °C. The dry film was ground with a mortar and pestle and the powder was stored in a desiccator for at least 1 week before testing. This sample was labeled as WG25ED. An identical WG sample, but made without adding EDTAD, was prepared as reference material and labeled WGenRef.

**Synthesis of WG25ED4GEN:** A sample was prepared in the same way as WG25ED, but after the EDTAD acylation (2 h), the suspension temperature was raised to 50 °C. Thereafter, 4 wt% of GEN, relative to the WG content, was added to the suspension. The suspension was left under stirring at 50 °C for 2.5 h (Figure 2-2). Then, the pH was adjusted to 3.5 (1 M HCl) and the suspension centrifuged

at 3900 RCF, 5 min (Figure 2-3). The SN was replaced by fresh MQW and the suspension with the pellet was shaken for ≈5 min at 2000 rpm. The mixture was subsequently neutralized using 1 M NaOH to pH ≈7.5. The cleaned and neutralized mixture was poured into a Petri dish and dried overnight at 40 °C. The obtained film (Figure 2-4) was ground with a mortar and pestle and then placed in a desiccator with silica gel for a minimum of 1 week before testing. This sample was labeled WG25ED4GEN.

**Synthesis of WG4GEN25ED:** The sample was prepared in a way similar to WG25ED, but after denaturing the WG suspension, the temperature of the suspension was lowered to 50 °C. Then, 4 wt% of GEN relative to the WG content was added to the suspension and the temperature was kept at 50 °C for 2.5 h (Figure 2-1). Thereafter, the temperature was lowered to RT and the EDTAD was used to acylate the WG as described for WG25ED. The cleaning and drying process also followed the procedure of WG25ED. The sample was labeled WG4GEN25ED. An identically treated sample, but without adding EDTAD, labeled WG4GEN, was prepared as a reference to WG4GEN25ED. A summary of all the sample description, yield, and nitrogen content is given in Table 2.

**Swelling Measurements:** The FSC of the samples was determined using the standard procedure according to Non-Woven Standard Procedure (NWSP) 240.0.R2, also known as the “teabag” test.<sup>[70]</sup> An amount of 150 mg of the dry materials was added to nonwoven fabric bags having a dimension of 40 × 60 mm<sup>2</sup> and a minimum of 400 mesh. The bags containing the materials were hooked on a rod and immersed in a beaker containing MQW or 0.9 wt% NaCl solution. The saline solution was used to simulate body fluids. The immersion times were 60, 300, 600, 1800, and 86 400 s (24 h). For the removal of the excess liquid, the bags were hung for 10 s outside the liquid and then placed on a paper towel for 10 s before weighing. The swollen weight was measured in triplicate per sample type. Three prepared empty bags were handled identically and immersed in MQW or saline for 24 h to obtain an average correction factor ( $W_b$ ). The swelling was calculated according to Equations (1 and 2):

$$W_b = W_s / W \quad (1)$$

$$FSC = \frac{[W_i - (W_o \cdot W_b)] - W_d}{W_d} \quad (2)$$

where  $W_s$  and  $W$  are the weights of the wet and dry blank bags, respectively.  $W_i$  is the weight of the swollen material,  $W_o$  the weight of the dry bag used and  $W_d$  the weight of dry powder added.

To evaluate the performance of the materials for sanitary applications, defibrinated sheep blood was also used as a testing liquid, using a swelling time of 30 min. The results are the average of duplicates and the standard deviation is reported.

For determining the liquid retention of the swollen materials, a centrifuge retention capacity (CRC) test was performed. An amount of ≈150 mg of the protein powder was placed in a teabag and swollen in the test liquid for 30 min, as described in the FSC test. Then the bags, containing the swollen material, were deposited on a metal mesh sheet to support the bag and centrifuged at 1230 rpm (250 RCF) for 3 min. The weight of the bags after the centrifugation was recorded. The CRC was determined on triplicates using Equation (3). A correction factor for the empty bags was also determined and calculated using Equation (1).

$$CRC = \frac{(W_c - (W_o \cdot W_b) - W_d)}{W_d} \quad (3)$$

where  $W_c$  is the weight of the bags containing the material after the centrifugation and  $W_b$  the correction factor for CRC.

**SE-HPLC:** SE-HPLC was performed on a Waters 2690 separations module and a Waters 996 photodiode array detector (Waters, USA) using a Biosep-SEC-S4000 (300 × 4.5 mm) with a prefilter SecurityGuard GFC 4000 (Phenomenex, USA). A three-step extraction procedure was implemented as reported by Gällstedt et al.<sup>[71]</sup> for evaluating the

extractability of the proteins and their fractions. A solution of 0.5 wt% SDS and 0.05 M NaH<sub>2</sub>PO<sub>4</sub> (pH 6.9) was always used as an extraction buffer. An amount of 16 mg of each material was dispersed in 1.3 mL of the SDS-phosphate buffer and shaken at 2000 rpm for 5 min. The dispersion was then centrifuged at 16 000 RCF for 30 min and the SN decanted (Ext. 1). For obtaining the SN of the second extraction (Ext. 2), the pellet from Ext. 1 was resuspended in fresh SDS-phosphate solution (1.3 mL), ultrasonicated at an amplitude of 5 μm for 30 s, and then centrifuged as before and the SN decanted. For the third extraction (Ext. 3), 1.2 mL of fresh buffer was added to the pellet from Ext. 2 and repeated ultrasonication steps (30 + 60 + 60 s) were applied to the suspension with cooling to RT between sonication. The suspension was then centrifuged and the SN decanted (Ext. 3). The analysis was performed in triplicates.

The total protein extractability (all 3 extractions) of the as-received WG powder was used as a reference as well as the normalization value for the rest of the analyzed materials. A 0.2 mL min<sup>-1</sup> isocratic flow of a 50/50 mixture of 0.1% trifluoroacetic acid (TFA) MQW solution and 0.1% TFA acetonitrile solution was used as the mobile phase throughout. A total of 20 μL of the SNs from Ext. 1, 2, and 3 was injected onto the column. 3D chromatograms were recorded between 190 and 220 nm and extracted at 210 nm, which was integrated into two fractions: polymeric proteins (PP, from 8 to 18.5 min) and monomeric proteins (MP, from 18.3 to 30 min).

To follow the reaction products of EDTAD and GEN in the absence of WG, the reagents were reacted in alkaline conditions following the reactions process for WG25GEN and WG4GEN, respectively. In addition, GEN was also added to a reacted EDTAD solution following the reaction process as described for WG25ED4GEN. The solutions were lyophilized for 72 h and the resulting powders dissolved in MQW (3 mg 600 μL<sup>-1</sup>). The solutions were then diluted with 50% methanol and centrifuged at 6200 RCF for 15 min. A total of 2 μL of the individual SN was injected on an Agilent 1260 Infinity II HPLC system, equipped with a Quaternary Pump VL, a UV Diode Array Detector, and an LC/MSD detector (Agilent Technologies, USA). The column was an ACE Phenyl (50 × 3 mm, 3 μL) (VWR, UK). The solutions of the reacted EDTAD (rxEDTAD), reacted GEN (rxGEN), and the EDTAD/GEN (rxEDTAD/GEN) were eluted (at 40 °C) at a rate of 1 mL min<sup>-1</sup> using an acetonitrile gradient (10% acetonitrile to 97% acetonitrile + 0.1% TFA/MQW).

**FTIR:** FTIR spectra were obtained using a Perkin–Elmer Spectrum 400 (Norwalk, USA) coupled to a Golden Gate unit single-reflection ATR and a triglycine sulphate (TGS) detector (Graseby Specac LTD, England). All scans were obtained using a step and resolution of 1.0 and 4.0 cm<sup>-1</sup>, respectively, with 32 consecutive scans per sample. All spectra were normalized to the –CH<sub>2</sub> asymmetric stretching vibration band at 2926 cm<sup>-1</sup>.<sup>[72,73]</sup> The peak deconvolution was performed as reported by Cho et al.<sup>[24]</sup> using Perkin–Elmer Spectrum software (version 10.5.1 (2015)) using an enhancement factor (γ) of 2 and a smoothing filter of 70%.

**FE-SEM:** A S-4800 field emission scanning electron microscope (FE-SEM) (Hitachi, Japan) was used for studying the particle morphology before and after swelling. A voltage of 3 kV was used in all cases. The particles were put onto carbon tape and sputtered with a palladium/platinum (Pt/Pd) target in an Agar High-Resolution Sputter Coater 208RH (Agar Scientific, UK). The sputtering time for all samples was 45 s with an estimated conductive coating layer of 2 nm. For the analysis of the swollen particles, the teabags containing the swollen material (24 h of immersion) were frozen at –80 °C and lyophilized for 72 h. Then, the now foam-like material was carefully removed from the bags, submerged in liquid nitrogen and cryo-fractured. The particle size of the dry materials was calculated as the average of 50 particles using ImageJ.<sup>[74]</sup>

**TGA:** The thermal degradation behavior of the WG samples was evaluated using a TGA/SDTA 851 instrument (Mettler-Toledo, Switzerland). For the analysis, 14.5 ± 0.6 mg of the sample powder was put in 70 μL alumina crucibles. The thermal profile consisted of a drying step of 10 min at 50 °C and then a heating ramp from 50 °C to 800 °C at a heating rate of 10 °C min<sup>-1</sup>. A 50 mL min<sup>-1</sup> nitrogen flow was used during all tests.

**NMR:** Nuclear magnetic resonance (NMR)  $^1\text{H}$ -, 2D correlation spectroscopy (COSY), and nuclear overhauser effect spectroscopy (NOESY) were recorded at room temperature with a Bruker Avance III HD 400 MHz instrument with a BBFO probe equipped with a Z-gradient coil for structural analysis (Bruker, UK). The data were processed with MestreNova (Mestrelab Research) using 90° shifted square sine-bell apodization window; baseline and phase correction was applied in both directions.

**MALDI-TOF-MS:** MALDI-TOF-MS was conducted on a Bruker UltraFlex MALDITOF-MS equipped with a Scout-MTP Ion Source and an  $\text{N}_2$  laser (337 nm) (Bruker Daltonics, Germany). DHB and sodium solution were used as a matrix and a counter-ion, respectively.

## Supporting Information

Supporting Information is available from the Wiley Online Library or from the author.

## Acknowledgements

VINNOVA is acknowledged for the funds provided for this project (2015-03506), together with the collaboration of Lantmännen ek för and Essity AB, Sweden. Maria Luisa Prieto Linde is acknowledged for her assistance during the SE-HPLC analysis. Dr. Annelie Moldin is acknowledged for the feedback regarding the raw materials provided within the project. Hüsamettin Özeren is acknowledged for kindly providing the rendered protein molecular models. Boyang Guo is acknowledged for the kind assistance during the LC/MS analysis.

## Conflict of Interest

The authors declare no conflict of interest.

## Keywords

cross-linking, functionalization, proteins, superabsorbents, sustainability

Received: May 4, 2020

Revised: June 17, 2020

Published online: July 14, 2020

- [1] A. J. Capezza, W. R. Newson, R. T. Olsson, M. S. Hedenqvist, E. Johansson, *ACS Sustainable Chem. Eng.* **2019**, 7, 4532.
- [2] M. J. Zohuriaan-Mehr, K. Kabiri, *Iran. Polym. J.* **2008**, 17, 451.
- [3] S. Damodaran, *U.S. Patent* 6,310,105, **2001**.
- [4] D.-C. Hwang, S. Damodaran, *J. Appl. Polym. Sci.* **1996**, 62, 1285.
- [5] A. A. Cuadri, C. Bengoechea, A. Romero, A. Guerrero, *Eur. Polym. J.* **2016**, 85, 164.
- [6] A. J. Capezza, *Novel Superabsorbent Materials Obtained from Plant Proteins*, Sveriges Lantbruksuniversitet, Alnarp **2017**, pp. 1–54.
- [7] S. Damodaran, *U.S. Patent* 6,821,331, **2004**.
- [8] B. Zhang, Y. Cui, G. Yin, X. Li, Y. You, *Int. J. Polym. Mater.* **2010**, 59, 1018.
- [9] E. Johansson, A. H. Malik, A. Hussain, F. Rasheed, W. R. Newson, T. Plivelic, M. S. Hedenqvist, M. Gällstedt, R. Kuktaite, *Cereal Chem. J.* **2013**, 90, 367.
- [10] J. H. Woychik, J. A. Boundy, R. J. Dimler, *J. Agric. Food Chem.* **1961**, 9, 307.
- [11] A. J. Capezza, D. Glad, H. D. Özeren, W. R. Newson, R. T. Olsson, E. Johansson, M. S. Hedenqvist, *ACS Sustainable Chem. Eng.* **2019**, 7, 17845.
- [12] A. A. Cuadri, A. Romero, C. Bengoechea, A. Guerrero, *Polym. Test.* **2017**, 58, 126.
- [13] A. A. Cuadri, A. Romero, C. Bengoechea, A. Guerrero, *J. Polym. Environ.* **2018**, 26, 2934.
- [14] G. Rathna, S. Damodaran, *J. Appl. Polym. Sci.* **2001**, 81, 2190.
- [15] G. Rathna, S. Damodaran, *J. Appl. Polym. Sci.* **2002**, 85, 45.
- [16] D.-C. Hwang, S. Damodaran, *J. Agric. Food Chem.* **1996**, 44, 751.
- [17] D.-C. Hwang, S. Damodaran, *J. Am. Oil Chem. Soc.* **1997**, 74, 1165.
- [18] G. Rathna, J. Li, S. Gunasekaran, *Polym. Int.* **2004**, 53, 1994.
- [19] H. Rasel, T. Johansson, M. Gällstedt, W. R. Newson, E. Johansson, M. S. Hedenqvist, *J. Appl. Polym. Sci.* **2016**, 133, 42442.
- [20] P. Hernández-Muñoz, R. Villalobos, A. Chiralt, *Food Hydrocolloids* **2004**, 18, 647.
- [21] B. Alander, A. J. Capezza, Q. Wu, E. Johansson, R. T. Olsson, M. S. Hedenqvist, *Ind. Crops Prod.* **2018**, 119, 41.
- [22] Q. Wu, S. Yu, M. Kollert, M. Mtimet, S. V. Roth, U. W. Gedde, E. Johansson, R. T. Olsson, M. S. Hedenqvist, *ACS Sustainable Chem. Eng.* **2016**, 4, 2395.
- [23] Q. Wu, R. L. Andersson, T. Holgate, E. Johansson, U. W. Gedde, R. T. Olsson, M. S. Hedenqvist, *J. Mater. Chem. A* **2014**, 2, 20996.
- [24] S. W. Cho, M. Gällstedt, E. Johansson, M. S. Hedenqvist, *Int. J. Biol. Macromol.* **2011**, 48, 146.
- [25] B. S. Chiou, H. Jafri, T. Cao, G. H. Robertson, K. S. Gregorski, S. H. Imam, G. M. Glenn, W. J. Orts, *J. Appl. Polym. Sci.* **2013**, 129, 3192.
- [26] A. J. Capezza, M. Lundman, R. T. Olsson, W. R. Newson, M. S. Hedenqvist, E. Johansson, *Biomacromolecules* **2017**, 18, 1709.
- [27] A. J. Capezza, Q. Wu, W. R. Newson, R. T. Olsson, E. Espuche, E. Johansson, M. S. Hedenqvist, *ACS Omega* **2019**, 4, 18257.
- [28] C. Marquié, *J. Agric. Food Chem.* **2001**, 49, 4676.
- [29] U.S. Department of Labor, Occupational Safety and Health Administration, *Best Practices for the Safe Use of Glutaraldehyde in Health Care*. Labor, CreateSpace Independent Publishing, Platform, CA, USA **2006**, pp. 1–48.
- [30] M. F. Butler, Y.-F. Ng, P. D. A. Pudney, *J. Polym. Sci., Part A: Polym. Chem.* **2003**, 41, 3941.
- [31] F. Song, L.-M. Zhang, *Ind. Eng. Chem. Res.* **2009**, 48, 7077.
- [32] L. Cui, J. Jia, Y. Guo, Y. Liu, P. Zhu, *Carbohydr. Polym.* **2014**, 99, 31.
- [33] H.-C. Liang, W.-H. Chang, K.-J. Lin, H.-W. Sung, *J. Biomed. Mater. Res.* **2003**, 65A, 271.
- [34] S. Wu, H. Dong, Q. Li, G. Wang, X. Cao, *Carbohydr. Polym.* **2017**, 168, 147.
- [35] C. Ninh, A. Iftikhar, M. Cramer, C. J. Bettinger, *J. Mater. Chem. B* **2015**, 3, 4607.
- [36] H. Tonami, H. Uyama, S. Kobayashi, K. Rettig, H. Ritter, *Macromol. Chem. Phys.* **1999**, 200, 1998.
- [37] K. Tsuchiya, K. Numata, *ACS Macro Lett.* **2017**, 6, 103.
- [38] R. Hollertz, V. L. Durán, P. A. Larsson, L. Wågberg, *Cellulose* **2017**, 24, 3883.
- [39] R.-M. P. Karlsson, P. T. Larsson, P. Hansson, L. Wågberg, *Biomacromolecules* **2019**, 20, 1603.
- [40] W. Brostow, H. E. Hagg, *Materials Recycling and Sustainability, in Materials: Introduction and Applications*, Vol. 1, John Wiley & Sons, New Jersey, USA **2017**, pp. 427–440.
- [41] K. Pal, A. T. Paulson, D. Rousseau, in *Modern Biopolymer Science* (Eds. S. Kasapis, I. T. Norton, J. B. Ubbink), Academic Press, San Diego, USA **2009**, pp. 519–557.
- [42] Y. Wang, F. Bamdad, Y. Song, L. Chen, in *Encapsulation Technologies and Delivery Systems for Food Ingredients and Nutraceuticals* (Eds. N. Garti, D. J. McClements) Woodhead Publishing, Cambridge, UK **2012**, pp. 412–450.
- [43] V. Bhagat, M. L. Becker, *Biomacromolecules* **2017**, 18, 3009.

- [44] A. S. Nashef, D. T. Osuga, H. S. Lee, A. I. Ahmed, J. R. Whitaker, R. E. Feeney, *J. Agric. Food Chem.* **1977**, 25, 245.
- [45] I. Olabarrieta, S.-W. Cho, M. Gällstedt, J.-R. Sarasua, E. Johansson, M. S. Hedenqvist, *Biomacromolecules* **2006**, 7, 1657.
- [46] N. H. Ullsten, S. W. Cho, G. Spencer, M. Gällstedt, E. Johansson, M. S. Hedenqvist, *Biomacromolecules* **2009**, 10, 479.
- [47] K. A. Tilley, R. E. Benjamin, K. E. Bagorogoza, B. M. Okot-Kotber, O. Prakash, H. Kwen, *J. Agric. Food Chem.* **2001**, 49, 2627.
- [48] F.-L. Mi, S.-S. Shyu, C.-K. Peng, *J. Polym. Sci., Part A: Polym. Chem.* **2005**, 43, 1985.
- [49] A. Barth, *Biochim. Biophys. Acta, –Bioenerg.* **2007**, 1767, 1073.
- [50] S. Krimm, J. Bandekar, in *Advances in Protein Chemistry*, Vol. 38 (Eds. C. B. Anfinsen, J. T. Edsall, F. M. Richards), Academic Press, London, UK **1986**, pp. 181–364.
- [51] J. J. Nájera, A. B. Horn, *Phys. Chem. Chem. Phys.* **2009**, 11, 483.
- [52] J.-J. Max, C. Chapados, *J. Phys. Chem. A* **2004**, 108, 3324.
- [53] F.-L. Mi, H.-W. Sung, S.-S. Shyu, *J. Polym. Sci. Part A: Polym. Chem.* **2000**, 38, 2804.
- [54] R. S. Lanigan, T. A. Yamarik, *Int. J. Toxicol.* **2002**, 21, 95.
- [55] C. Chang, B. Duan, J. Cai, L. Zhang, *Eur. Polym. J.* **2010**, 46, 92.
- [56] K. C. Lanigan, K. Pidsosny, *Vib. Spectrosc.* **2007**, 45, 2.
- [57] R. C. Horton, T. M. Herne, D. C. Myles, *J. Am. Chem. Soc.* **1997**, 119, 12980.
- [58] C. Lievens, D. Mourant, M. He, R. Gunawan, X. Li, C.-Z. Li, *Fuel* **2011**, 90, 3417.
- [59] S. Di Tommaso, P. David, K. Picolet, M. Gabant, H. David, J.-L. Moraçais, J. Gomar, F. Leroy, C. Adamo, *RSC Adv.* **2013**, 3, 13764.
- [60] P. Slusarewicz, K. Zhu, T. Hedman, *Nat. Prod. Commun.* **2010**, 5, 1853.
- [61] K. Zhang, Y. Qian, H. Wang, L. Fan, C. Huang, A. Yin, X. Mo, *J. Biomed. Mater. Res., Part A* **2010**, 95A, 870.
- [62] J. Coates, in *Encyclopedia of Analytical Chemistry* (Ed: R. A. Meyers), John Wiley & Sons Ltd., Chichester **2006**.
- [63] Y. Liu, Z. Cai, L. Sheng, M. Ma, Q. Xu, Y. Jin, *Carbohydr. Polym.* **2019**, 215, 348.
- [64] H. M. C. Azeredo, K. W. Waldron, *Trends Food Sci. Technol.* **2016**, 52, 109.
- [65] D. Jagadeesh, D. J. P. Reddy, A. V. Rajulu, *J. Polym. Environ.* **2011**, 19, 248.
- [66] G. H. Robertson, T. K. Cao, K. S. Gregorski, W. J. Hurkman, C. K. Tanaka, B. S. Chiou, G. M. Glenn, W. J. Orts, *J. Appl. Polym. Sci.* **2014**, 131, 1.
- [67] Q. Wu, V. H. Lindh, E. Johansson, R. T. Olsson, M. S. Hedenqvist, *Ind. Crops Prod.* **2017**, 97, 184.
- [68] United Nations Department of Public Information, Information Sustainable Development Goals, <https://sustainabledevelopment.un.org/?menu=1300> (accessed: June 2020).
- [69] Q. Wu, H. Sundborg, R. L. Andersson, K. Peuvot, L. Guex, F. Nilsson, M. S. Hedenqvist, R. T. Olsson, *RSC Adv.* **2017**, 7, 18260.
- [70] Edana, Nonwovens Standard Procedures, Association of the Non-woven Fabrics Industry, NC, USA **2015**, pp. 1–13.
- [71] M. Gällstedt, A. Mattozzi, E. Johansson, M. S. Hedenqvist, *Biomacromolecules* **2004**, 5, 2020.
- [72] J. V. Gulmine, P. R. Janissek, H. M. Heise, L. Akcelrud, *Polym. Test.* **2002**, 21, 557.
- [73] E. Andreassen, in *Polypropylene. Polymer Science and Technology Series*, Vol. 2 (Ed. J. Karger-Kocsis), Springer, Dordrecht **1999**.
- [74] C. T. Rueden, J. Schindelin, M. C. Hiner, B. E. DeZonia, A. E. Walter, E. T. Arena, K. W. Eliceiri, *BMC Bioinf.* **2017**, 18, 529.